Fabrication of Human Genomic DNA Encapsulated Supermacroporous Alginate (SMPA) Beads

Ramona Pasandideh

Submitted to the
Institute of Graduate Studies and Research
in partial fulfillment of the requirements for the degree of

Doctor of Philosophy
in
Chemistry

Eastern Mediterranean University
September 2020
Gazimağusa, North Cyprus

Approval of the Institute of Graduate Studies and Research

Prof. Dr. Ali Hakan Ulusoy
Director

I certify that this thesis satisfies all the requirements as a thesis for the degree of Doctor of Philosophy in Chemistry.

Prof. Dr. İzzet Sakallı
Chair, Department of Chemistry

We certify that we have read this thesis and that in our opinion it is fully adequate in scope and quality as a thesis for the degree of Doctor of Philosophy in Chemistry.

Assoc. Prof. Dr. Kerem Teralı
Co-Supervisor

Prof. Dr. Mustafa Gazi
Supervisor

Examining Committee

1. Prof. Dr. Mustafa Gazi
2. Prof. Dr. Ferhan Girgin Sağın
3. Prof. Dr. Okan Sirkecioğlu
4. Prof. Dr. OsmanYılmaz
5. Assoc. Prof. Dr. Hayrettin Ozan Gülcan

ABSTRACT

In this study, human genomic DNA (hDNA) encapsulated alginate cryogel beads (SMPA) and normal alginate beads were fabricated via freeze-thawing cryogelation and microinjection procedures respectively. The fabricated beads were characterized by scanning electron microscopy (SEM) and fluorescent microscope. The characterization results showed that both beads exhibited smooth surfaces with obvious pores and burgled topologies, however, a bug-like sprout is visibly seen on the surface of SMPA beads. Also, the encapsulated hDNA showed brilliant green fluorescence when visualized with fluorescence microscopy.

The encapsulation efficiency of 89.1−96.7% was achieved when the concentration of hDNA and alginate varied within 0.05−0.075% and 0.5−0.75 wt%, respectively in the presence of 0.1 M $CaCl_2$ crosslinking agent. ~80% hDNA was released over an extended period of 80 h when SMPA was immersed in a 0.5 M Na_2HPO_4 solution diluted with 10 mM Tris buffer (pH 7). The SMPA cryobeads demonstrated a higher swelling capability when compared with the normal beads. In the first 3 h, SMPA cryobeads achieved 225% swelling ratio compared with the normal beads that attained 155%. Beyond 3 h, the normal beads did not show significant swelling ratio while SMPA increased obviously to 315% before reaching equilibrium at the tenth hour.

Results and trends here demonstrated that the fabricated supermacroporous alginate-based cryogel beads have great potential to be used as a biocompatible vehicle for transporting biomacromolecules.

Keywords: controlled release systems; human genomic DNA; alginate polymeric cryobeads; supermacroporous; gene therapy

ÖZ

Bu çalışmada, insan genomik DNA'sı (hDNA) kapsüllenmiş aljinat kriyojel boncuklar (SMPA) ve normal aljinat boncuklar, sırasıyla dondurarak çözme kriyojelasyon ve mikroenjeksiyon prosedürleriyle üretildi. Üretilen boncuklar, taramalı elektron mikroskobu (SEM) ve floresan mikroskobu ile karakterize edildi. Karakterizasyon sonuçları, her iki boncuğun da bariz gözeneklere ve soyulmuş topolojilere sahip pürüzsüz yüzeyler sergilediğini, ancak SMPA boncuklarının yüzeyinde gözle görülür şekilde böcek benzeri bir filizlenme görüldüğünü gösterdi. Ayrıca kapsüllenmiş hDNA, floresan mikroskobu ile görüntülendiğinde parlak yeşil floresan ışıma göstermiştir.

0,1 M $CaCl_2$ çapraz bağlayıcı madde varlığında hDNA ve aljinat konsantrasyonu ağırlıkça sırasıyla % 0,05 - 0,075 ve % 0,5 - 0,75 arasında değiştiğinde % 89,1 - 96,7'lik kapsülleme verimliliği elde edildi. SMPA, 10 mM Tris tamponu (pH 7) ile seyreltilmiş 0.5 M Na_2HPO çözeltisi içerisinde 80 saatlik uzun bir süre boyunca bekletilmesi sonucu ortama ~% 80 oranda hDNA salınmıştır. SMPA kriyoboncukları, normal boncuklarla karşılaştırıldığında daha yüksek bir şişme kapasitesi sergiledi. İlk 3 saatte SMPA kriyoboncukları % 155'e ulaşan normal boncuklara kıyasla% 225 şişme oranına ulaştı. 3 saatten sonra, normal boncuklar önemli şişme oranı göstermezken, SMPA onuncu saatte dengeye ulaşmadan önce % 315 şişme oranına yükseldi.

Buradaki sonuçlar ve eğilimler, üretilmiş olan süper gözenekli aljinat bazlı kriyojel boncuklarının biyomakromoleküllerin taşınması için biyo-uyumlu bir araç olarak kullanılmak için büyük bir potansiyele sahip olduğunu göstermiştir.

Anahatar kelimeler: kontrollü salım sistemleri; insan genomik DNA'sı; aljinat polimerik kriyoboncuklar; süper gözenekli; gen tedavisi

ACKNOWLEDGMENT

First, I would like to express my feeling to my supervisor Prof. Dr. Mustafa Gazi who has a great talent for supervising me during my Ph.D. thesis. Also, I would like to thank my mighty co-supervisor Assoc. Prof. Dr. Kerem Teralı who supports me in all parts of the biological experiments. Besides, Assoc. Prof. Dr. Akeem Oladipo helped me a lot during my journey.

I wish to express my heartfelt thanks to my unique parents that tolerate my absence during these years and support me not only during my Ph.D. but also in all steps of my life. And last but not the least, I would like to declare my deepest feeling to my lovely sister, who is more than the sister but more like a consultant, a real friend and everything for me.

TABLE OF CONTENTS

LIST OF TABLES

LIST OF FIGURES

Chapter 1

INTRODUCTION

Gene therapy is a promising therapeutic approach recently adopted to effectively treat many challenging and acquired incurable disorders. This has been canvassed as a breakthrough in molecular medicine. Unfortunately, its application in vivo is inhibited due to difficulties in transportation of negatively charged molecules like DNA, fragile and biomacromolecules into the nucleus without degradation. Even after the delivery of these biomolecules to the patient, they are still vulnerable to degradation; and thus require protection to assure potency and maintain integrity. To overcome these constraints, an encapsulation strategy in a suitable controlled delivery vehicle has been adapted. The controlled release vehicles have become the focal point for various material scientists and biomedical industries; because they can maintain the biomacromolecules (such as nucleic acids, proteins and peptides) concentration within the cellular microenvironment, inhibit their degradation and reduce toxicity to nontarget cells and provide a sustained release to target.

Recent reports have shown that various materials have been evaluated as a delivering carrier for controlled release of biomolecules. For instance, Zoe et al. [1] synthesized laminated magnetic hydroxyapatite (LM-HAp)/DNA nanohybrid via an intercalation protocol and characterized the lamellar HAp-based biological vehicle. Considering the gel electrophoresis analysis, the authors revealed that the lamellar HAp demonstrated immense potential for gene therapy and protected the DNA from the degradation of

DNase I. Viral carriers have long been employed for delivering DNA due to their high efficiency; unfortunately, reports have indicated that those vectors can trigger dangerous immunological responses, limited by the cost of production, DNA cargo size; and largely confined by the risk of carcinogenesis and mutagenesis [2,3].

Non-viral gene delivery vehicles like polymer-based carriers (chemical vectors) are particularly attractive alternative due to their safety profile, shelf stability, biocompatibility, ease of fabrication, controlled chemical diversity and various modifiable functional groups. Also, the majority of these polymers are hydrophilic, have conventional net charges suitable for cellular uptake, possess stimuli sensitive functionalities and biodegradable links. Numbers of polymeric materials have been employed for biomedical applications. For instance, polymeric-based injectable hydrogels have demonstrated substantial success as promising vehicles for delivery of biomolecules; unlike the pre-formed hydrogels, Wang and coworkers [4] reported that these injectable polymeric hydrogels can be formed in vivo and can easily be delivered to inaccessible sites or regions that are difficult to access during surgery. Thereby, providing greater biomolecules concentration at the desired target location while limiting accumulation in non-targeted parts of the body. Similarly, Wang et al [5] reported the synthesis of chitosan-gelatin-based microgel for sustained folic acid delivery, they concluded that the cost-effective injectable microgels exhibited sufficient potential to be used as a delivery vehicle for hydrophobic bioactive molecules [2,4].

However, the majority of the polymers are not applicable for biomedical applications because they do not fulfil the criteria of biomaterials; such as the non-generation of toxic fragments or products, biodegradability, biocompatibility [2,6]. It is worthy to

mention that the structure of polymeric vehicles plays an important role in encapsulation and transfection efficiency. Researchers reported that low-molecular-weight polymers demonstrated better DNA unpackaging with less cytotoxicity, while high-molecular-weight polymeric materials exhibited greater DNA binding and improved cellular uptake [2,7]. In general, cationic polymers electrostatically bind with the negatively charged DNA and form polyplex (DNA/polymer complex) which can pass through the cell membrane into the cell; and the encapsulated DNA may be released when the pH at the desired site is triggered [2]. According to Deng et al. [8], lower transfection efficiency was achieved with the high molecular weight polyethyleneimine (400-kDa) disulphide compared with the low-molecular-weight (7-kDa) disulphide transfected cells, also the 7-kDa carrier showed less cytotoxic. Olden et al, synthesized cationic polymer, poly (2-dimethylaminoethyl methacrylate, pDMAEMA) based carrier for gene delivery to both primary human T and cultured cells; they reported sufficient transfection with efficiencies ~50% in the Jurkat human T cell with less concomitant toxicity, that is >90% viability. It is worthy to mention that polymeric hydrogels have been applied extensively in various biomedical applications due to their ability to hold a substantial amount of water within the polymeric chains [2,9].

In this work, we explored the feasibility of encapsulating human DNA (hDNA) into calcium alginate-based supermacroporous cryobeads prepared via microinjection and freeze-thawing cryogelation protocol. Alginate is a seaweed-based negatively charged polysaccharide, that can form a gel in the presence of calcium in an aqueous solution [10]; and widely used for biomedical applications due to its non-toxicity, bioadhesive nature, abundance and biocompatibility [11].

Unmaredkar et al. fabricated chitosan-alginate polyelectrolyte complex bead as a controlled delivery polymeric vehicle for calcium channel blocker (cilnidipine). According to their in vitro dissolution study, a stable controlled release of 89.6% cilnidipine was achieved over 12 h; and they concluded that the alginate-based beads can be utilized for extending the release of drugs having a lower half-life [2,11].

Also, Goldshtein et al. [12] reported electrostatically driven self-assembled Ca^{2+} alginate-sulphate nanomaterial as a transfection agent for intracellular plasmid DNA delivery. According to their report; the alginate-based non-viral vector did not induce lymphocyte activation, showed cytocompatibility and provided a decent delivery rate (34%) of the plasmid to the nucleus. The alginate hydrogelling ability has expanded their research perspectives and application uses in biomedicine, and have been reported to provide a good matrix for the entrapment of biomolecules and as an efficient delivery vehicle of DNA both in vitro and in vivo for gene therapy [2,13].

Here, the preparation protocol employed for the fabrication of the alginate-based biomaterial is facile even though the alginate has a similar charge with the polyanionic DNA. We considered the high sensitivity of the biomolecules towards mild intracellular conditions; hence, the structural integrity of the SMPA (supermacroporous alginate) beads was examined by scanning electron microscopy and fluorescence microscopy. The incorporated hDNAs were visualized by the fluorescence microscopy after staining the SMPA beads with ethidium bromide fluorescent probe. The swelling properties of SMPA cryobeads and normal alginate incorporated hDNA beads were investigated; SMPA beads achieved sufficiently high (89.1-96.7%) hDNA encapsulation efficiency with sustained-release profiles over 80 h [2].

1.1 Deoxyribonucleic Acid (DNA)

Early in the1860s, the chemical composition of the nucleus was studied by Friedrich Miescher who was a chemist. He started to collect the cells and cracked them with the pepsin enzyme. As a result, he observed the special structure exactly in the centre of the nucleus. He conducted chemical investigations on the chemical structure of the nuclei; he discovered that it's composed of carbon, oxygen, nitrogen, and a high amount of phosphorus. He isolated the first deoxyribonucleic acid (DNA) in 1869 and the DNA molecular structure was identified by Francis Crick and James Watson in 1953. DNA is a vital long biopolymer made from repeating units called nucleotides. Each nucleotide structure contains a sugar group, phosphate group and a nitrogen base (Figure 1). Adenine (A), guanine (G), cytosine (C) and thymine (T) are four different types of DNA bases [14]. According to the acidic area of the nucleus, it is called nucleic acid.

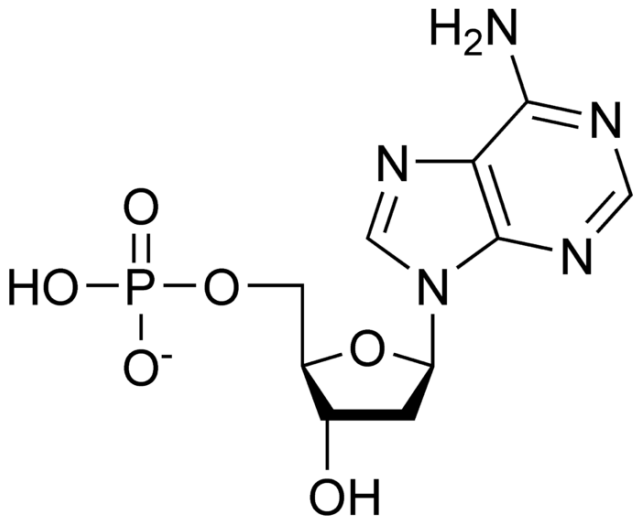

Figure 1: The common nucleotide structure in the DNA molecule

DNA is supercoiled double helix located in the nucleus bound to each other by hydrogen bonds between different bases. H-bonds typically play a crucial role in biological molecules dimensional form. So, there are three H-bondings between G and C bases, and two H-bonds between T and A (Figure 2) [14].

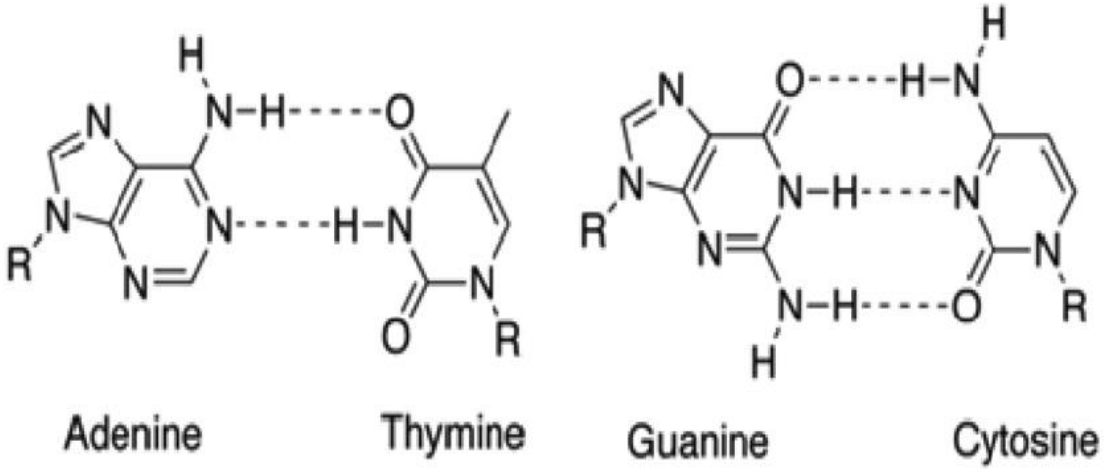

Figure 2: Chemical structure and hydrogen bonding between Adenine-Thymine, and Guanine-Cytosine pairing.

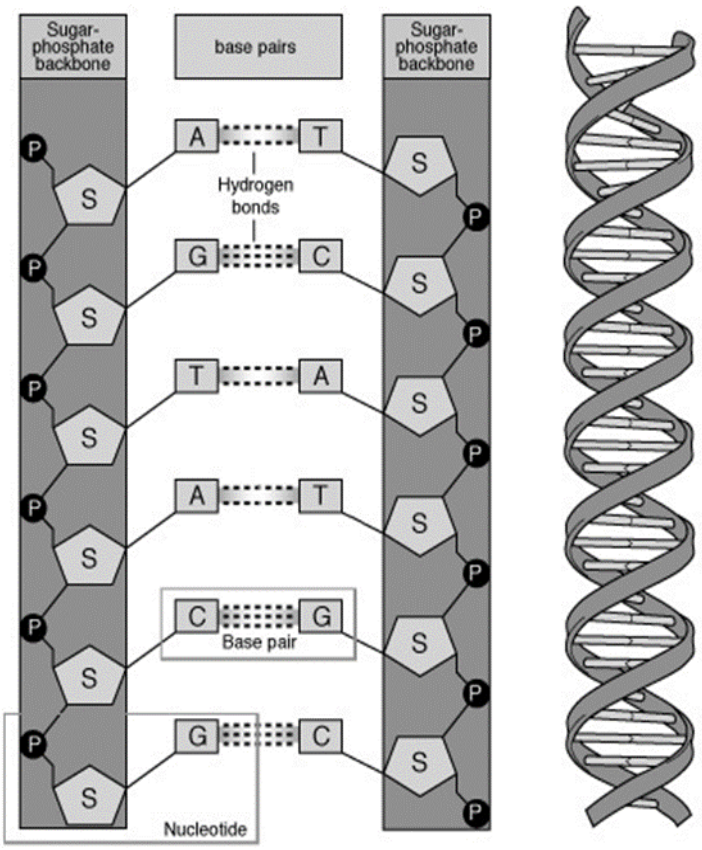

Figure 3: The covalent structure of the double-stranded DNA molecule

Adenine and guanine are classified as purine, which are heterocyclic aromatic compounds with double rings. Also, cytosine and thymine are pyrimidines with only one ring. These are the repetitive bases through the structure of the double-helical DNA molecule (Figure 3). Also, each strand of DNA has a specific direction from 5' to 3' or the opposite direction from 3' to 5'. Furthermore, transcription and translation start their activities according to the direction of each strand and the specific sequence of DNA. Transcription is the first step of gene expression to make some single strand of an RNA molecule from DNA and translation is the last step of preparation of protein molecules. Besides, early in 1940, E. Chargaff applied chromatography to find out the ratio of the bases through DNA macromolecule. As a result, he found that the number of moles of A is equal to the number of T, also C amount is the same as G [15].

The hereditary genetic transfer from a nucleotide which is located in DNA molecule to the amino acids in a protein structure follows two significant steps. The first step is known as the transcription and the second step is the translation. In the first step of transcription, DNA double-stranded molecule changes to the RNA single strand inside the nucleus of all eukaryotic cells. Then, in the translation step, this RNA molecule changes to the protein to express the specific gene inside the cytoplasm of the cell. In the process, messenger RNA (mRNA), transfer RNA (tRNA), ribosomal RNA (rRNA) and small nuclear RNA (snRNA) are the most important types of RNA molecules for the transcription and the following translation processes. Transcription consists of three main steps which are named as initiation (RNA polymerase binds to the specific region of DNA molecule to start transcription), elongation (RNA polymerase unwind double strand of DNA molecule and transcription of template single strand of DNA continues by base pairing) and finally the last step which is termination (the specific region of DNA as a template signals to stop transcription process) [16].

Translation will be the second process to produce mature proteins which have important functions in the human body. It has also three main steps as initiation (start codons signal to start the translation), elongation and termination (stop codon signals to stop the translation process). The immature proteins are ready but are not capable to be used for their specific application. It means that some modifications and post modifications should apply to these immature proteins to make them mature according to their use in the human body [17].

1.2 Human Genome

The entire set of nucleic acid sequences are named as the human genome and this is encoded as DNA inside the 23 chromosomes placed in the cell nucleus. The genomic DNA can be extracted from human blood cells by using the special extraction kit [18]. Human gDNA extraction was first carried out in 1869 and till then it has very significant applications in molecular and genetics biology fields of study. The original source of gDNA extracted is the whole blood sample. There are different methods to extract and purify gDNA, but most of them are based on the same steps. Lysate preparation, binding, washing and eluting human gDNA are three consecutive steps of DNA extraction from blood cells, which needs to use some special enzymes and buffers to reach the pure source of gDNA [19].

1.3 Polymerase Chain Reaction (PCR)

Early in 1980, this momentous technique was presented by Cary Mullis. PCR has expanded rapidly according to its advantages and applications in the molecular biology field. Nowadays it is performed as the routine technique by the computer automatically. It is the technique to prepare several DNA fragments from a particular section of the pattern in vitro. PCR is exactly similar to DNA replication. DNA polymerase is the specific enzyme for applying replication step by using one strand of DNA from 3'to 5' direction as a pattern and make another single strand with 5' to 3' direction. Also, the enzyme needs one identifier fragment for starting replication. Denaturation is the first step of the PCR technique, which is based on heating to make single-stranded DNA (ssDNA) from double-stranded DNA (dsDNA). Annealing is the next step, which is going to make these double strands again by cooling them [2]. Presence of a primer is essential for starting the replication. According to the structure of DNA (which is double-stranded), two primers should exist. Those primers are

responsible to find out the exact location of the gene that is needed to replicate and determine the size of the replicated fragments [20]. The identified fragments bind to two different locations of DNA, and DNA polymerase starts to replicate all the fragment between these two parts. So, it can determine the length of replicated DNA in this way. Master-mix should be prepared by mixing pattern DNA, primers, nucleotide triphosphate and DNA polymerase in a test tube. Then the master-mix is heated to separate double strands of DNA to make a single strand. Afterwards, by decreasing the temperature, primers are able to bind to the strands. The replication starts with DNA polymerase. After the required time, the system is heated again to make separated fragments and cool down for primer binding. So, at the end of this step, 4 specific transcripts of DNA prepared. The system heated again to make 8 copies. Then, 16 transcripts and continue to make more copies from the pattern fragment. In general, 2^n repeats are prepared after n cycles. Gel electrophoresis by ethidium bromide staining is then applied to observe replicated fragments of DNA [21].

1.4 Electrophoresis

Electrophoresis is used to separate macromolecules according to their sizes. The technique applies a negative charge so proteins move towards a positive charge. Electrophoresis is extensively utilized in biochemistry, biotechnology, molecular biology, clinical chemistry and genetics for the purification and visualization of macromolecules. Generally, electrophoresis is employed extensively in DNA, RNA and protein analysis; it can be used to regain required fragments of DNA via agarose gel. Gel electrophoresis based on agarose is a beneficial method for DNA fragments separation into different sizes ranging between 100 bp to 25 kb [22]. In this technique, there are positive and negative charges on both sides of the tank. According to the

location of phosphate groups on each strand of DNA backbone, DNA has a negative charge. So, DNA strands start to migrate from negative charge to the positive charge by the application of the electric field. As a result, the lighter fragments will migrate faster than the heavier ones. Finally, the gel is observed under UV light to compare all the DNA fragments with the first line, which belongs to the ladder [20,23].

Chapter 2

LITERATURE RIVIEW

2.1 Polymeric Materials

A polymeric material is a substance or material made up of very large molecules, or macromolecules, consisting of a variety of subunits that are repeated. Both synthetic and natural polymers play important and ubiquitous roles in daily life due to their large range of properties. Polymers range from common synthetic plastics such as polystyrene to natural biopolymers like DNA and biological structure and function-fundamental proteins. Polymers, both synthetic and natural, are formed by the polymerization of various small molecules, called monomers. The primary emphasis of polymer science has been the products resulting from the linkage of recurring units by covalent chemical bonds. Polynucleotides, polypeptides and polysaccharides are three important types of biopolymers. Protein synthesis requires multiple enzyme-mediated procedures to transcribe genetic information from DNA to RNA and then translate that information from amino acids to synthesize the protein specified. Polymer properties depend on their structure and they are divided into different classes according to their physical basis. Indeed, Synthetic polymers are used in almost all aspects of life presently. Low density, good thermal/electrical insulation properties, low cost of fabrication, low-energy demanding polymer manufacture and facile processing into final products are their unique properties [24].

2.2 Polymeric Hydrogels

Hydrogels are three-dimensional hydrophilic polymers with the ability to maintain a large amount of water. They can swell and hold a considerable amount of water without being dissolved. The presence of hydrophilic functional groups like -OH, -COOH, $-NH_2$, -CONH, $-CONH_2$ and $-SO_3H$ cause the hydrophilicity of the network. They are cross-linked polymeric network formed by the fundamental reaction of one or linkage of more monomers. Therefore, they can be applied as primary candidates in tissue engineering for biosensors, vectors for drug delivery and carriers or matrices for cells [24]. The water mass fraction in a hydrogel, usually in the swelling stage, is much greater than the polymer mass fraction. Normally synthetic polymers are used according to their solubility in water in the non-cross-linked form to achieve a high degree of swelling [25,26].

Polymer hydrogels are materials with viscoelastic features and, network structure caused by cross-linker and the solvent, according to their priority. Recently, polymer hydrogels have been used in ordinary life in various forms such as shampoo, soap, hair gel, toothpaste and also as a contact lens. Also, some advanced industrial usage of polymer hydrogels is found in pharmaceutical, textile, agriculture industries, and water treatment areas [27]. Hence, gel materials are one of the utmost popular compounds in our daily life nowadays. These gels are different conforming to needed usage like body care gels is not similar to oil recovery application or agriculture. Indeed, Hydrogels have many applications in biomedical fields like in hygiene products, contact lenses and wound dressings. Some commercial application of hydrogels is in tissue engineering and drug delivery [27].

2.3 Sodium Alginate

Sodium alginate (NaC6H7O6) is a linear polysaccharide derived from alginic acid comprised of 1, 4-β-d-mannuronic (M) and α-l-guluronic (G) acids. The cell wall component of marine brown algae consists of almost 30 to 60% alginic acid. The transformation of alginic acid to sodium alginate improves its solubility in water, which helps its extraction. Its liquid–gel manner in aqueous solutions is one of the benefits of the alginate form. When monovalent sodium ions are changed to divalent ions like calcium, the reaction occurs almost instantly, moving from a solution with low viscosity to a gel structure. The gel content is a copolymer made up of monomer components of two forms [28].

There is much application of alginate in engineering and biomedical sciences due to its desirable features such as ease of gelation and biocompatibility. Sodium alginate hydrogels have been applied in tissue engineering, drug delivery and wound healing. Sodium alginate is the form of sodium salt from alginic acid [25,28].

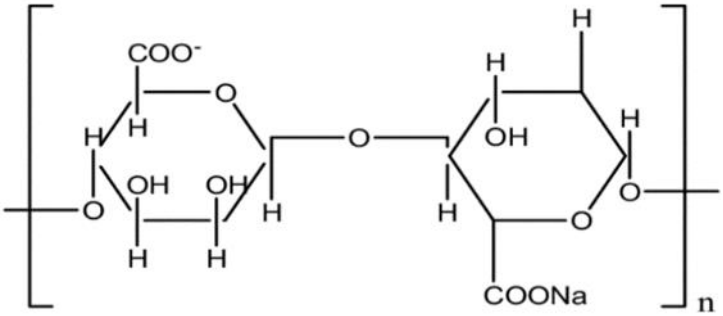

Figure 4: The structure of sodium alginate

2.4 Biomolecule Delivery and Gene Therapy

Recent molecular biological developments with the conclusion of the Human Genome Project have developed a genetic understanding of biological processes and pathogenesis of diseases. The targets for therapeutic approaches have been identified for various genes involved in disease and cell processes. Over the past few years, both the number of human genes specifically related to disease states and the variety of vector systems available to express such genes for medical reasons have grown remarkably. Therapeutic gene therapy is a biological substance that has the following features. It contains an active material containing or consisting of transgenic nucleic acid used throughout human administration to control, fix, substitute, add or remove a genetic sequence. Also, its medicinal, prophylactic or therapeutic impact is directly linked to the transgenic nucleic acid sequence found therein or even to the genetic expression result of that sequence. The most critical, and toughest, difficulty in gene therapy is delivery. A delivery system is required which first has to overcome the extracellular barriers like targeting particular tissues or cells and protecting from degradation, and cellular barriers such as cellular absorption, endosomal escape, nuclear entry and nucleic release afterwards. Efficient, accurate, long-lasting and stable should be an ideal gene delivery vector. Gene delivery systems contain both viral vectors and non-viral vectors. Viral vectors are the most effective carriers, but their use is limited by their small size of the DNA that they carry and their immunogenicity. Non-viral vectors are safer, reproducible, less costly and have no size limit on DNA. The biggest weakness of non-viral vector is their weak transfection performance, however different techniques have improved it, and the attempts are still ongoing. Non-viral delivery developments have potentially led to an increased number of drugs approaching clinical trials [28].

Chapter 3

MATERIALS AND METHOD

3.1 Materials

Analytical grade reagents are used in this research. Sodium alginate (molecular weight of ~ 120 kDa), calcium chloride, ethylenediaminetetraacetic acid (EDTA) and agarose powder were obtained from Sigma-Aldrich (USA). Fluorescent dye 1% solution in water, proteinase K, RNase and genomic lysis/binding buffer were purchased from Invitrogen (Thermo Fisher Scientific, USA).

3.2 Human DNA Extraction

3.2.1 Lysate Preparation

The DNA extraction procedures were adapted from the previously reported procedures [29] and slightly modified. Firstly, 200 mL of defrosted blood was added to a fresh microtube and 20 μL of proteinase K was mixed with it. Afterwards, 20 μL of RNase and 200 μL of genomic lysis/binding buffer were added to the above mixture and vortexed gently at 55 C°for 20 min. Finally, 200 μL of EtOH (ethanol) was added and vortexed rapidly to obtain the lysate [30].

3.2.2 hDNA Binding and Elution

640 μL freshly prepared lysate was added to lysis/binding buffer and ethanol in a tube and centrifuged at 10,000 rpm for 1 min. The sample was then poured into a new tube and washed twice consecutively with a 500 μL buffer, then centrifuged for 3 min at 10,000 rpm. The sample was poured into a sterile microcentrifuge tube and 1 μL genomic elution buffer was added. Then, the tube was incubated at room temperature for 1 min and centrifuged at 10,000 rpm for 1 min at room temperature. Finally, purified hDNA was obtained and a second elution procedure was performed to increase the DNA recovery. Obtained purified human DNA (hDNA) was stored at 4 °C for a short term application or -20 °C for long term storage [31].

3.2.3 Polymerase Chain Reaction and Gel Electrophoresis

The PCR master mix was prepared by mixing 0.3 μL forward primer (F-primer), 0.3 μL reversed primer (R-primer), 2 μL genomic DNA and 22.4 μL sterile distilled water. All samples were taken out of the laminar flow cabinet to the thermal cycler (PCR machine). Then, subjected to 35 cycles. Three main steps of polymerization were followed. The first step is denaturation that was applied at 95°C for 30 seconds. Two strands of DNA separated from each other and many DNA-single strands were obtained. Annealing was the next step that helps forward and backward primers to bind to the single strands by cooling down at 57°C for 30 seconds. The final step involves extension at 72°C for 45 seconds, resulting in the polymerization of the second strand. These 3 steps were repeated for 35 times and gel electrophoresis was applied afterwards. 1 g agarose powder was added to 50 mL buffer (Tris base, boric acid, EDTA) and mixed gently in microwave flask. The solution was poured gradually to avoid making any bubbles, which causes to disrupt the gel. Any bubbles could be removed by a pipette tip within the gel tank. Rapidly, the gel was kept at 4°C about

10-15 min or the gel was left to sit at room temperature for about 20 min to become entirely solidified[32].

The Ladder was injected as a guide into the first well, g-DNA into the 2nd well, PCR product into the 3rd well and primer into the 4th well (Table 1). Then, the gel was run at 80-150 V until the dye line is approximately 75-80% of the way down the gel. Finally, the gel was placed into the container, which was filled with EtBr for staining, and placed on a rocker for 20-30 min. The EtBr solution was replaced with water and de-stained for 5 min. In the end, the DNA fragments were visualized by a UV transilluminator (Picture 2) [32].

Table 1: Different length of DNA samples preparation for applying gel electrophoresis

EtBr	**Different length of DNA**	**Distilled water**	**Total volume**
1 µL	0.5 µL DNA ladder	8.5 µL	10 µL
1 µL	8.5 µL genomic DNA	0.5 µL	10 µL
1 µL	5 µL PCR product	4 µL	10 µL
1 µL	5 µL primer	4 Ml	10 µL

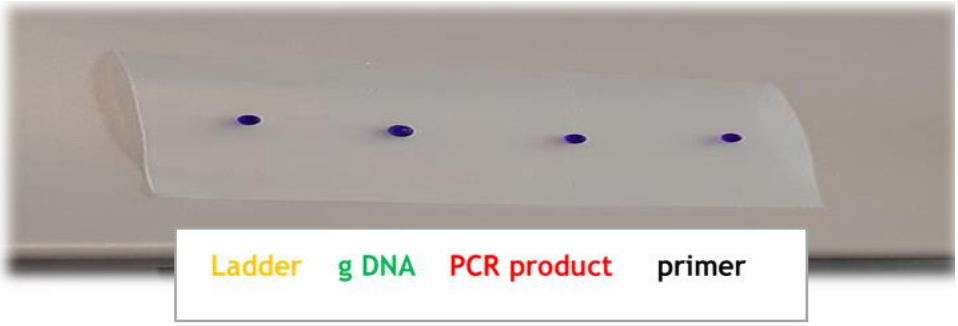

Figure 5: Electrophoresis samples preparation

Figure 6: Gel electrophoresis visualization under UV light

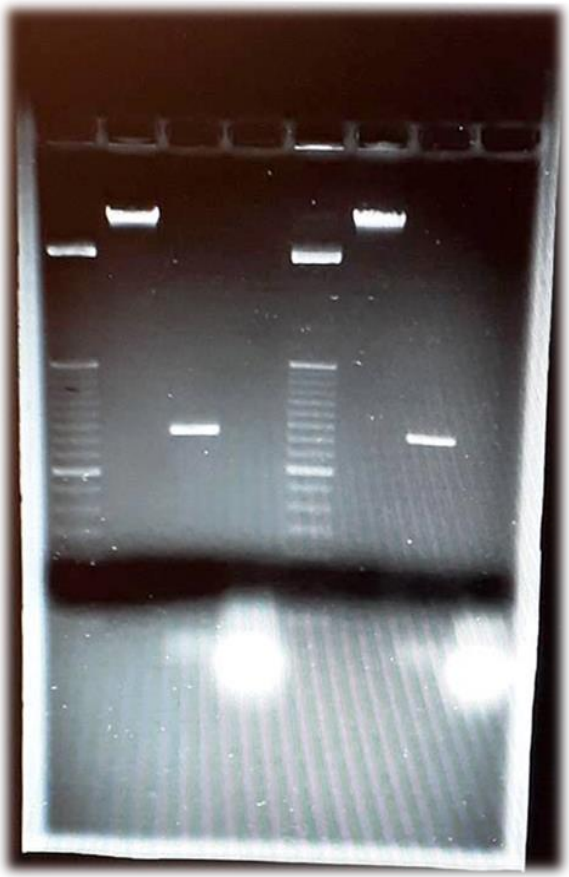

Figure 7: Sample gel electrophoresis visualization result

3.3 Encapsulation of hDNA

3.3.1 Supermacroporous Alginate (SMPA) Beads

SMPA was produced via a facile approach (shown in Figure 5) using microsyringe with a needle diameter of 0.5 mm. Initially, an aqueous solution of 0.5% (w/w) alginate was mixed with 0.05% (w/w) purified hDNA; the mixture was well stirred to ensure homogeneity at room temperature and then, cooled to 5 ℃. The cooled mixture was injected dropwise at 2 mL/min flow rate into a freshly prepared 0.1 M $CaCl_2$ and stirred at 150 rpm for cryogelation. The crosslinked beads were stirred for 60 min, filtrated and deep-frozen at -20 ℃ overnight. Subsequently, the frozen beads were thawed at room temperature (subjected to three freeze-thawing cycles); and obtained cryogel beads are named SMPA and used for further application [2].

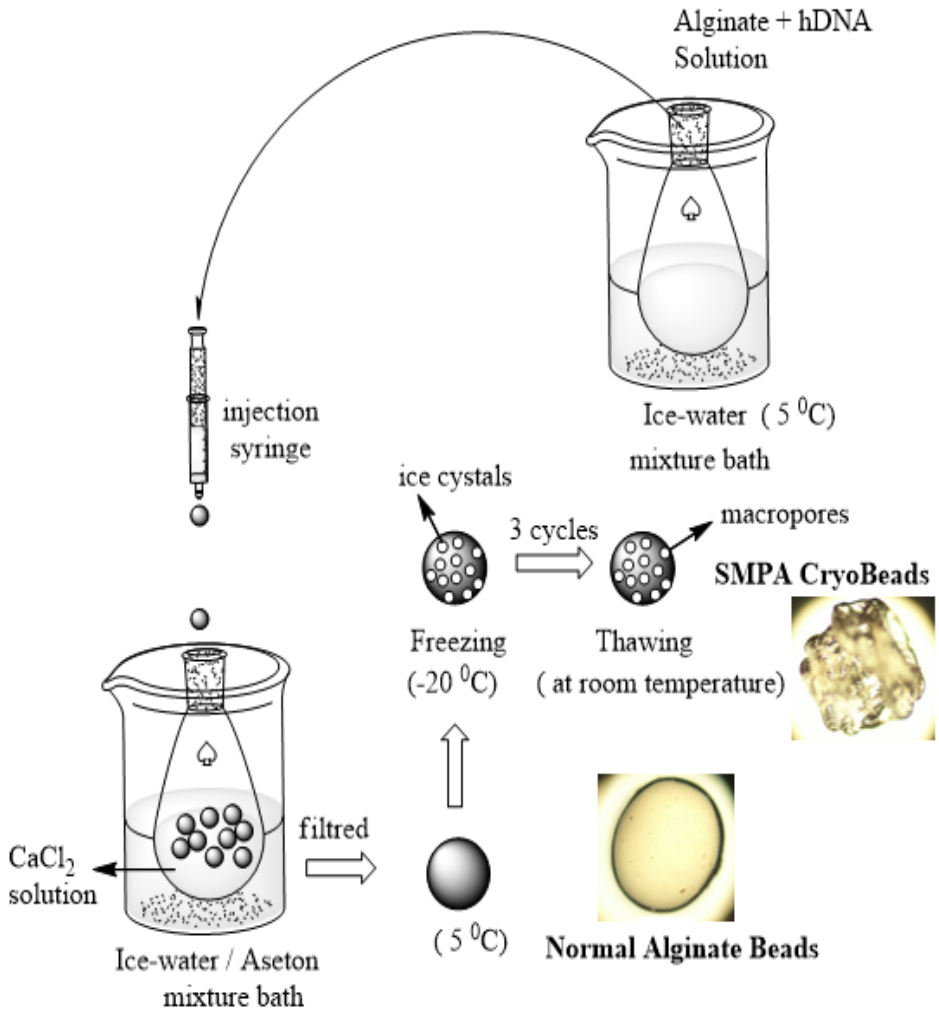

Figure 8: Schematic illustration of the preparation of SMPA beads by microinjection method under freezing condition

3.4 SEM Analysis of SMPA Beads

SMPA beads were characterised by scanning electron microscope (SEM) using an S-2500 C microscope (Hitachi, Japan) and fluorescent microscope (FM) using Zeiss AxioPhot epifluorescence microscope (Zeiss, Germany). For FM characterization, freshly fabricated SMPA cryobeads were stained with a solution of 1% fluorescent dye; then placed on a micro slide after 10 min equilibration and irradiated. The presence of hDNA in the SMPA beads was assessed visually using 10× objective lenses.

3.5 hDNA Loading and Encapsulation Efficiency

The amount of hDNA encapsulated during the fabrication procedure was determined using UV–vis spectrophotometer (T80 + PG Instruments Ltd., UK)) at a wavelength of 260 nm which is the maximum absorption peak of nucleic base chromophores since the alginate does not exhibit any absorbance. Firstly, the various concentration of alginate and hDNA presented in Table 2 were mixed as previously described. To release the hDNA; certain weights of SMPA beads were immersed in 5 mL of 0.5 M Na_2HPO, then diluted 10-fold by 10 mM Tris buffer (pH 7) and filtered to remove the calcium phosphate precipitate. The encapsulated hDNA in the filtrates was quantified by measuring its absorbance at 260 nm. The filtrates of alginate beads without DNA were utilised as blanks and the encapsulation efficiency (EE%) was calculated as follows [33].

$$EE\% = \frac{detected\ amount\ (mg) of\ hDNA\ in\ SMPA\ beads}{theoretical\ amount\ (mg) of\ hDNA\ in\ SMPA\ beads} \times 100 \quad (1)$$

3.6 Swelling Degree of the SMPA Beads

The preweighed amount of the dried SMPA beads and normal alginate beads containing hDNA (W0) were introduced into 20 mL 0.1 M phosphate buffer at 37 °C

± 0.2 °C (pH 7) solution separately. The swollen beads were removed from the medium at predetermined time intervals and gently blotted with filter paper to remove excess liquid from the surface of the swollen beads [2,33]. The weight of the swollen SMPA beads (W1) were taken and the swelling degree (S%) was calculated accordingly:

$$S\% = \left(\frac{W1 - W0}{W0} \right) \times 100 \quad (2)$$

3.7 In vitro hDNA Release Study

In vitro release was performed at 50 rpm in a thermostatic rotating shaker at 40°C to investigate the release kinetics of hDNA from the SMPA and normal alginate containing hDNA beads. The beads were immersed into 50 mL of phosphate buffer (pH 7) solutions; the concentration of the hDNA released was measured at the wavelength of 260 nm and the percentage of hDNA released was obtained considering the ratio of the mass of hDNA released at a known time to the equilibrium hDNA values in the buffer solutions.

3.8 Characterization Methods

Before applying infrared spectroscopy, 3 categories of beads were prepared with different ratios (a, b and c) according to Table 2 for both genomic and primer DNA. Also, 0.27 g $CaCl_2$ was added to the beads as cross-linker. Freshly DNA loaded hydrogels were stained with ethidium bromide (EtBr) for 10-15 minutes gently and destained with distilled water straightaway. The UV lamp was used to observe hydrogel beads. The fluorescent pictures of the beads were at 4×, 10× and 40× magnifications. The observation was performed at 25°C. Also, provide SEM information including the machine model.

3.9 DNA Release

UV spectroscopy was applied to the analysis of DNA release behaviour of both genomic DNA and primer DNA in EDTA, and NaCl solutions. Drawing the calibration curve before taking absorbance of the beads, is the first and foremost step. For this aim, solutions with 10 mM, 8 mM, 6mM, 4mM and 2mM concentrations were used for drawing calibration curve. So, the absorbance in the same wavelength for just buffer with NaCl and EDTA as the calibration curve (without beads) were taken. After that, both genomic and primer DNA were put into the NaCl and EDTA one by one to record the specific absorption.

Table 2: NaCl calibration curve absorbance at λ=223 nm

Concentration (mM)	Absorbance
10	0.886
8	0.709
6	0.507
4	0.336
2	0.492

Table 3: EDTA Calibration curve absorbance at λ=223 nm

Concentration (mM)	Absorbance
10 Mm	0.886
8 Mm	0.709
6 mM	0.507
4 mM	0.336
2 mM	0.492

Chapter 4

RESULTS AND DISCUSSION

4.1 Preparation of DNA Encapsulated Alginate-based Beads

Herein, we describe the complexation process of sodium alginate with DNA, mediated by calcium ion bridges to form slightly anionic beads. Below tables show three types of beads preparation with a different concentration ratio of NaAlg and both genomic and plasmid DNA.

Table 4: Preparation of three types of alginate beads, which encapsulated gDNA with different concentration amount a) Equal concentration of gDNA and NaAlg b) double concentration of NaAlg c) double concentration of gDNA

	a	**b**	**c**
gDNA	0.1 mL (100 µL)	0.1 mL (100 µL)	0.2 mL (200 µL)
NaAlg	0.005 g	0.1 g	0.05 g

Table 5: Preparation of three types of alginate beads, which encapsulated primer DNA with different concentration amount a) Equal concentration of gDNA and NaAlg b) double concentration of NaAlg c) double concentration of gDNA

	a	**b**	**c**
Primer	0.1 mL (100µL)	0.1 mL (100 µL)	0.2 mL (200 µL)
NaAlg	0.005 g	0.1 g	0.005 g

Table 6: Weight of each 3 different fractions of gDNA beads a) Equal concentration of gDNA and NaAlg b) double concentration of NaAlg c) double concentration of gDNA

Source of DNA	**a**	**b**	**c**
gDNA	0.0012 g	0.0017 g	0.002 g

Table 7: Weight of each 3 different fractions of primer beads a) Equal concentration of gDNA and NaAlg b) double concentration of NaAlg c) double concentration of gDNA

Source of DNA	**a**	**b**	**c**
Primer DNA	0.003 g	0.004 g	0.003 g

Table 8: The weight of 3 different beads encapsulated gDNA in EDTA in time a) Equal concentration of gDNA and NaAlg b) double concentration of NaAlg c) double concentration of gDNA

Time (min)	**a**	**b**	**c**
10	0.002 g	0.0037 g	0.0063 g
20	0.0042 g	0.0053 g	0.0071 g
30	0.0062 g	0.0064 g	0.0089 g
40	0.0074 g	0.008 g	0.0112 g
50	0.0088 g	0.0097 g	0.0132 g
60	0.01 g	0.01 g	0.0143 g
80	0.012 g	0.0132 g	0.0158 g
90	0.0144 g	0.0157 g	0.0245 g

Table 9: The weight of 3 different beads encapsulated primer DNA in EDTA in time. a) Equal concentration of gDNA and NaAlg b) double concentration of NaAlg c) double concentration of gDNA

Time (min)	**a**	**b**	**c**
10	0.0032 g	0.0125 g	0.009 g
20	0.0064 g	0.014 g	0.013 g
30	0.0087 g	0.0168 g	0.016 g
40	0.0091 g	0.0183 g	0.018 g
50	0.0094 g	0.0185 g	0.019 g
60	0.0099 g	0.021 g	0.02 g
80	0.013 g	0.0247 g	0.028 g
90	0.015 g	0.025 g	0.0125 g

Table 10: The weight of 3 different beads encapsulated gDNA in NaCl in time. a) Equal concentration of gDNA and NaAlg b) double concentration of NaAlg c) double concentration of gDNA

Time (min)	**a**	**b**	**c**
10	0.0024 g	0.0047 g	0.0031 g
20	0.0035 g	0.0061 g	0.0044 g
30	0.0038 g	0.0067 g	0.0058 g
40	0.0043 g	0.0073 g	0.0062 g
50	0.0051 g	0.0086 g	0.0067 g
60	0.006 g	0.0088 g	0.0071 g
80	0.0064 g	0.0099 g	0.0079 g

Table 11: The weight of 3 different beads encapsulated primer DNA in NaCl in time. a) Equal concentration of gDNA and NaAlg b) double concentration of NaAlg c) double concentration of gDNA

Time (min)	**a**	**b**	**c**
10	0.0082 g	0.0096 g	0.012 g
20	0.0091 g	0.012 g	0.015 g
30	0.0094 g	0.013 g	0.0171 g
40	0.012 g	0.0155 g	0.0184 g
50	0.016 g	0.0158 g	0.02 g
60	0.023 g	0.0171 g	0.023 g
80	0.044 g	0.0176 g	0.024 g

4.2 Characterization of the SMPA Beads

4.2.1 SEM and Microstructural Analysis of SMPA and Normal Alginate Beads

The morphologies of SMPA and normal alginate beads containing hDNA are shown in Figure 6(a,b). Both beads exhibited smooth surfaces with obvious pores and burgled topology. Notably, a bug-like sprout is visibly seen on the surface of SMPA cryogel beads which is compact with a crack-like surface. This may be attributed to the consecutive freeze-thawing processes and thus reduced its crosslinking density. Compared with the normal alginate beads, the sprout is smoother and homogenous. The smooth microstructure of the normal alginate beads containing hDNA is verified under the microscope as shown in Figure 6(d) and the sprout is well-distinct in Figure 6 (c) [2,33]. Also, the detailed porosities and average bead diameters are presented in Table 12. Note that SMPA cryogel beads are more porous compared with the normal SMPA beads with a greater pore size of 2.6 mm; this revealed that SMPA can encapsulate more hDNA and exhibits a higher degree of swelling.

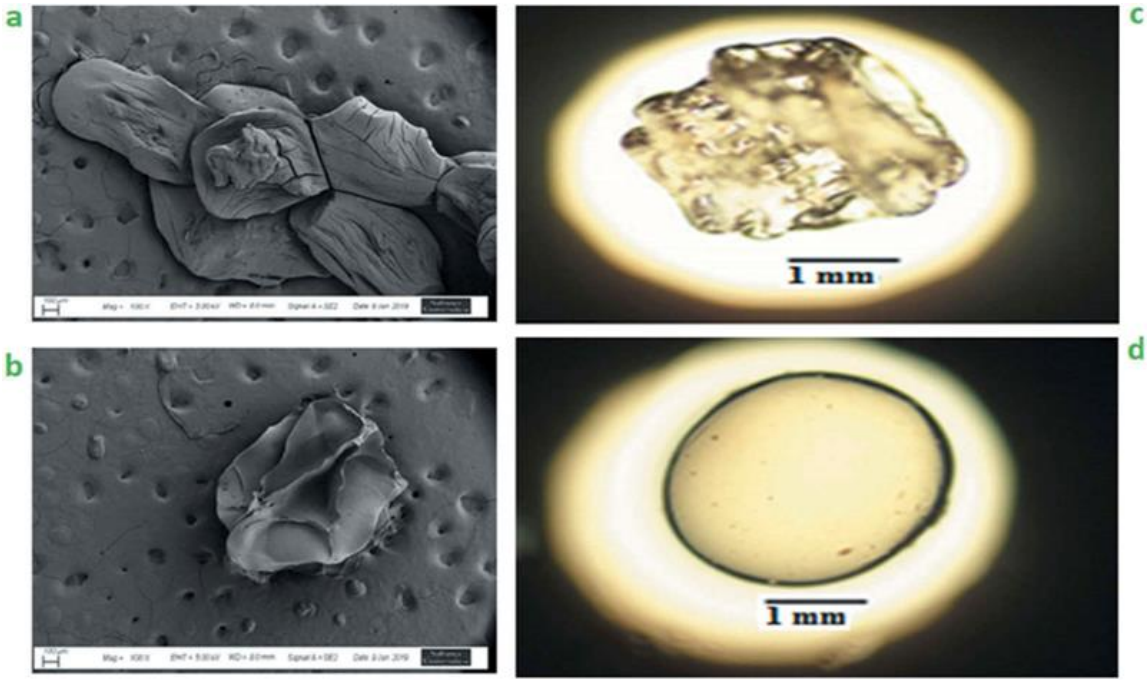

Figure 9: SEM morphology of (a) SMPA cryogel bead (b) normal SMPA bead; and microstructure of (c) SMPA cryogel bead (d) normal SMPA bead under light microscope at10x magnification

Table 12: Mean diameters of hDNA loaded SMPA beads under different conditions

Microtube diameter (mm)	Flow rate (mL/min)	$CaCl_2$ (M)	Temp (^{0} C)	Porosity (%)	Mean bead diameter (mm)
0.5	2	0.1	5	82.0 ± 1.1	2.1
0.5	2	0.1	−20	88.5 ± 1.1	2.6

4.2.2 Fluorescence Microscopy Analysis

The fluorescence microscopy in Figure 6 showed specific background fluorescence for 0.5% alginate with 0.05% incorporated hDNA. Staining of the SMPA bead with the 1% fluorescent probe enabled visualisation of the hDNA incorporated in the bead. The FM of alginate bead without hDNA is not expected to show background fluorescence (image not shown), as seen in Figure 7, SMPA containing hDNA exhibited a bright green fluorescence which confirms that the incorporated hDNA

retained its double-stranded structure. A similar observation has been reported by Machado et al. [34].

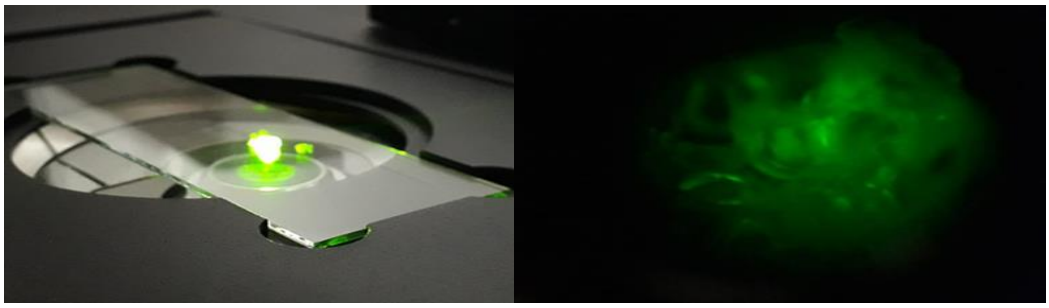

Figure 10: The fluorescent microscopy of SMPA beads at 40× magnification

4.2.3 FTIR Analyses

The infrared bands of the DNA, NaAlg, normal encapsulated DNA bead and cryo encapsulated DNA beads are shown in Figure 8. The characteristic peaks of the DNA are observed, specifically, the broad peak at 3232.25 cm^{-1} belong to a hydroxyl group, the phosphate antisymmetric and symmetric stretches are observed at 1208 and 1080 cm^{-1} and the base pair (protein) vibration is noticed at 1634 cm^{-1}. The characteristic peaks of the alginate are observed; the mannuronic acid functional group at wavenumber 816 cm^{-1} and the uronic acid at wavenumber 908 cm^{-1}, the OH functional group is observed at 3232 cm^{-1} and CH2 stretching at wavenumber 2945 cm^{-1}. The DNA encapsulated beads contained the characteristics peaks of the pristine materials with weaker peaks.

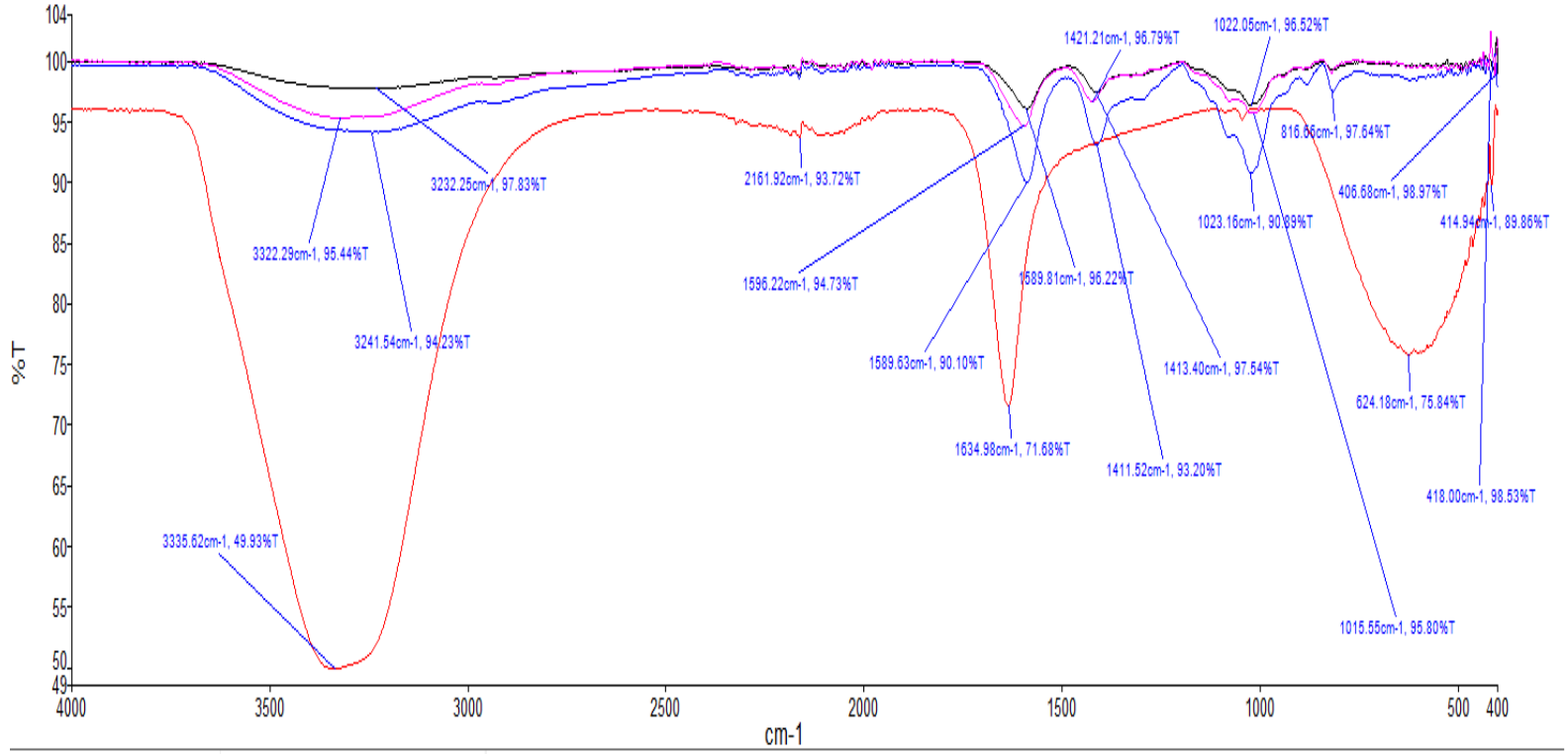

Figure 11: FTIR spectra of normal SMPA, cryo SMPA, DNA and NaAlg

4.3 Swelling Studies

Swelling kinetics is very important for biomolecule release since it controls the swollen gel dissolution [38]. SMPA swelling kinetics were studied and represented in Figure 9. Initially, the rate of buffer uptake increased rapidly for both types of beads sharply and, then levelled off. Particularly, in the first 3 h, SMPA cryobeads achieved 225% swelling ratio compared with the normal beads that attained 155%. The initial stage is a result of the rapid hydration of the SMPA beads which caused the formation of a gel layer, followed by bulk hydration, and then sharp swelling [36]. Beyond 3 hours, the normal beads did not show significant swelling ratio while SMPA increased obviously to 315% then reached equilibrium until 10th hour. The higher swelling ratio of SMPA is attributed to its higher porosity and lesser crosslinked density [2].

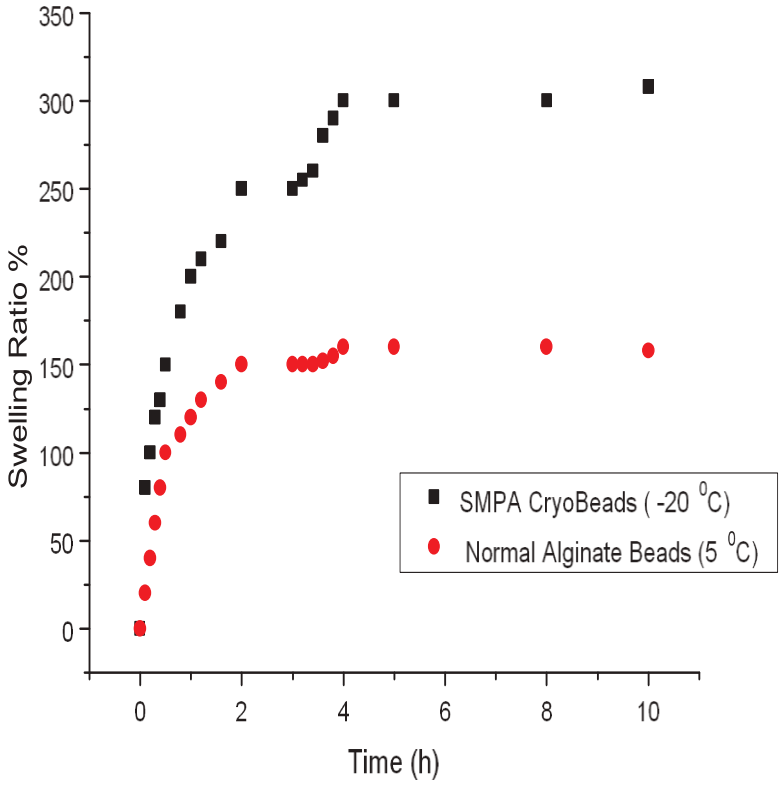

Figure 12: Swelling kinetics of the SMPA cryobeads and normal alginate beads

4.4 hDNA Encapsulation Efficiency in the SMPA Beads

SMPA cryobeads were dissolved in Na_2HPO_4 to quantify the hDNA incorporated in the cryobeads; the disodium phosphate sequestered the calcium ions in the cryobeads network to obtain calcium phosphate and, thus, disrupted the cryogel network [34]. Although the hDNA is a negatively charged polyanionic polymer just like the alginate; no phase separation due to net repulsive interaction was observed for the ranges of alginate concentration (0.5–0.75 wt %) and hDNA (0.05–0.075 wt %) used. Therefore, the retention of the negatively charged hDNA within the alginate network might be as a result of electrostatic attraction between the Ca^{2+} and the polyanionic hDNA. The encapsulation efficiency is presented in Table 13 and we found that the hDNA was efficiently encapsulated within the alginate network within the range of 89.1 to 96.7% which is similar to the values reported elsewhere using crosslinked alginate polymer [2,34].

Specifically, the encapsulation efficiency increased from 91.6 to 96.7% when the hDNA concentration was increased from 0.05 to 0.075 wt% in the presence of 0.5 wt% of alginate solution and 0.1 M $CaCl_2$. The encapsulation efficiency was noticed to be decreased when the concentration of alginate was further increased to 0.75 wt% which might be as a result of a higher concentration of alginate compared with the fixed amount of Ca^{2+}. Notably, no significant entrapment efficiency was observed when the alginate concentration was increased to 0.75 wt% in the presence of 0.075 wt.% hDNA in comparison to that of 0.5 wt.% alginate and 0.05 wt.% hDNA [2].

Table 13: Encapsulation efficiency of hDNA in SMPA cryobeads

Alginate (wt. %)	DNA (wt. %)	Encapsulation efficiency (%)
0.5	0.05	91.6
0.5	0.075	96.7
0.75	0.05	89.1
0.75	0.075	91.9

$CaCl_2$ is 0.1 M in each case

4.5 In vitro hDNA Release Kinetics

We assessed the release behaviour of the SMPA beads in a 0.5 M Na_2HPO solution diluted with 10 mM Tris buffer (pH 7). Visually SMPA beads exhibited a significant increase in volume sharply; and as shown in Figure 10, the hDNA released speed was very rapid in the first 20 h and faster for SMPA cryobeads which reached 70% hDNA release while the normal beads reached 50% release in the same timeframe. After the initial burst period, the hDNA release rate slowed down and SMPA beads maintained sustained release behaviour until 80 h. The hDNA release can be explained based on the fact that an increase in the osmotic pressure within the gel network occurred which resulted in a decrease in the effective cross-link density and release of the hDNA. The difference in the release behaviour of the SMPA cryobeads and normal alginate incorporated hDNA beads is attributed to the different physicochemical properties [40], i.e. the porosity and crosslink density [7,34].

The hDNA molecules diffused through the polymer pores after it was swollen and a large amount was released from SMPA cryobeads with larger pores (porosity of 88.5 ± 1.1) compared with the normal alginate beads where some of the encapsulated hDNA was retained due to lower pore size. The hDNA release data were modelled using the

power-law equation [38] to understand the mode of the hDNA release behaviour from the SMPA beads:

$$\frac{Mt}{M} = kt^n \quad (2)$$

Where Mt/M is the fraction of the hDNA released at the time t; k accounts for the structural properties of the beads and n reveals the mechanism of the hDNA release, when the values are 0.45, $0.45 < n < 0.89$, $0.89 < n < 1.0$ it reveals that the release system is Fickian diffusion-based, anomalous (non-Fickian) diffusion and zero-order mechanism, respectively [2,35]. The transport exponents for hDNA release from the SMPA cryobeads and normal alginate beads were 0.58 and 0.62 (Table 13), respectively, which reveals non-Fickian diffusion kinetics. Indicating that the hDNA release occurred via a comparable simultaneous swelling of the gels and relaxation of the alginate polymeric chains. Considering this trend, it is believed that SMPA beads exhibited sustained release behaviour with the potential to protect hDNA from external denaturants [2].

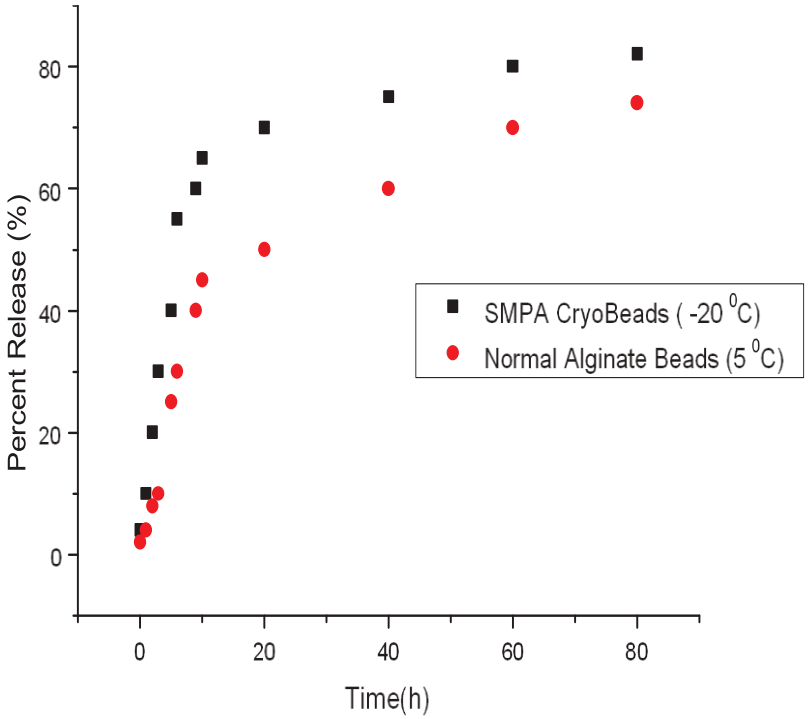

Figure 13: hDNA released kinetics of the SMPA beads and normal alginate beads

Table 14: Coefficient and exponents of hDNA release kinetics

Materials	K	N	R2
SMPA cryobeads (–20 °C)	28.6	0.58	0.99
Normal alginate beads (5 °C)	8.65	0.62	0.98

Table 15: gDNA in buffer + EDTA absorbance at different times

	NaAlg ⬆	DNA ⬆
T=30' λ=268 nm Abs=0.615 W=0.0061 g	T=30' λ=269 nm Abs=0.566 W=0.0066 g	T=30' λ=268 nm Abs=0.636 W=0.008 g
T=60' λ=268 nm Abs=0.695 W=0.012 g	T=60' λ=267 nm Abs=0.601 W=0.013 g	T=60' λ=267 nm Abs=0.680 W=0.015 g
T=120' λ=268 nm Abs=0.713 W=0.032 g	T=120' λ=268 nm Abs=0.733 W=0.038 g	T=120' λ=268 nm Abs=0.799 W=0.049 g
T=180' λ=268 nm Abs=0.852 W=0.045 g	T=180' λ=267 nm Abs=0.883 W=0.047 g	T=180' λ=268 nm Abs=0.914 W=0.056 g

Table 16: Primer DNA in buffer + EDTA absorbance at different times

	NaAlg⬆	DNA ⬆
T=30' λ=268 nm Abs=0.609 W=0.0088 g	T=30' λ=268 nm Abs=0.606 W=0.0151 g	T=30' λ=266 nm Abs=0.731 W=0.0163 g
T=60' λ=268 nm Abs=0.625 W=0.0099 g	T=60' λ=268 nm Abs=0.628 W=0.023 g	T=60' λ=268 nm Abs=0.680 W=0.015 g
T=120' λ=268 nm Abs=0.643 W=0.023 g	T=120' λ=268 nm Abs=0.691 W=0.0381 g	T=120' λ=268 nm Abs=0.799 W=0.049 g
T=180' λ=268 nm Abs=0.721 W=0.048 g	T=180' λ=268 nm Abs=0.728 W=0.051 g	T=180' λ=268 nm Abs=0.914 W=0.056 g

Table 17: gDNA in buffer + NaCl absorbance at different times

	NaAlg ⬆	DNA ⬆
T=30' λ=267 nm Abs=0.644 W=0.0041 g	T=30' λ=267 nm Abs=0.620 W=0.0073 g	T=30' λ=267 nm Abs=0.647 W=0.0063 g
T=60' λ=267 nm Abs=0.688 W=0.0061 g	T=60' λ=267 nm Abs=0.688 W=0.0084 g	T=60' λ=267 nm Abs=0.702 W=0.0072 g
T=120' λ=267 nm Abs=0.726 W=0.0146 g	T=120' λ=267 nm Abs=0.724 W=0.021 g	T=120' λ=267 nm Abs=0.783 W=0.0187 g
T=180' λ=267 nm Abs=0.797 W=0.0335 g	T=180' λ=267 nm Abs=0.883 W=0.0424 g	T=180' λ=267 nm Abs=0.891 W=0.0365 g

Table 18: Primer DNA in buffer + NaCl absorbance in different times

	NaAlg⬆	DNA⬆
T=30' λ=268 nm Abs=0.628 W=0.0097 g	T=30' λ=267 nm Abs=0.620 W=0.015 g	T=30' λ=268 nm Abs=0.648 W=0.0173 g
T=60' λ=268 nm Abs=0.712 W=0.024 g	T=60' λ=268 nm Abs=0.736 W=0.0182 g	T=60' λ=268 nm Abs=0.762 W=0.031 g
T=120' λ=268 nm Abs=0.773 W=0.044 g	T=120' λ=268 nm Abs=0.786 W=0.056 g	T=120' λ=268 nm Abs=0.804 W=0.048 g
T=180' λ=268 nm Abs=0.824 W=0.068 g	T=180' λ=268 nm Abs=0.866 W=0.074 g	T=180' λ=268 nm Abs=0.885 W=0.072 g

So, the weight and absorbance of both gDNA and primer DNA were checked in both EDTA and NaCl solution by time. As the result, when DNA concentration encapsulated by sodium alginate bead was increased, the absorbance number was also increased for both gDNA and primer DNA at 268 nm (third column of each table). In contrast, the beads with higher amount of NaAlg showed lesser absorbance number at the same wavelength (second column of each table).

Chapter 5

CONCLUSION

Many challenging and acquired incurable disorders have been treated *via* gene therapy and it has been canvassed as a breakthrough in molecular medicine. However, the transfer of fragile biomolecules like DNA has been a great constraint for gene therapy since the DNA is vulnerable to degradation. To solve this issue, an encapsulation of the DNA into a polymeric host has been adopted as a viable approach because they can maintain the biomacromolecules concentration within the cellular microenvironment, inhibit their degradation and provide a sustained release to target.

This study is directed towards the fabrication of alginate-based beads for encapsulation of human genomic DNA (hDNA). Particularly, alginate-based supermacroporous cryogel beads and normal alginate beads were fabricated via facile microinjection and cryocross-linking techniques. The alginate cryogel beads (SMPA), normal alginate beads and beads loaded with hDNA were characterized by Fourier transform infrared spectroscopy, scanning spectroscopy and fluorescence spectroscopy. Characteristics peaks of alginate and DNA were detected in the individual and beads-loaded spectra and the loaded DNA was validated by the fluorescence spectroscopy; revealing successful loading of the hDNA in the polymeric host.

The hDNA encapsulation efficiency of 89.1–96.7% was achieved for both beads and their release behaviour were sustained over 80 hours via non-Fickian diffusion-

controlled kinetics. The initial stage rapid hydration of the beads followed by bulk hydration, and then sharp swelling. Specifically; in the initial stage, the rate of buffer uptake increased rapidly for both types of beads then levelled off. SMPA cryobeads achieved 225% swelling ratio in 3 hours when compared with the normal beads that attained 155%.

Results herein demonstrated that SMPA cryobeads are a potential biomaterial for controlled release of biomacromolecules. Notably, SMPA beads are a better candidate for DNA encapsulating because they are more porous compared with normal alginate beads with a pore size of 2.6 mm. Also, SMPA exhibited higher swelling capacity due to its higher porosity and lesser cross-linked density. The results herein demonstrated the potential of the as-synthesized alginate-based supermacroporus beads for gene delivery system. Further research will be directed towards optimizing various factors influencing the DNA release, swelling kinetics and release behaviour in a controlled medium.

REFERENCES

[1] G. F. Zuo, Y. Z.Wan, Hou, X.F. Zeng, Y. Shen, G. J. Gao., Intercalative nanohybrid of DNA in laminated magnetic hydroxyapatite, *Mater. Technol.*, 30 (2014) 86-89.

[2] R. Pasandideh, M. Gazi, K. Teralı, and A. A. Oladipo, Fabrication of human genomic DNA encapsulated supermacroporous alginate beads, *Mater. Technol*., (2020) 1–8.

[3] J. Gao, T. Bergmann, W. Zhang, M. Schiwon, E. Ehrke-schulz, and A. Ehrhardt, Viral Vector-Based Delivery of CRISPR / Cas9 and Donor DNA for Homology-Directed Repair in an In Vitro Model for Canine Hemophilia B, *Mol. Ther.*, 14 (2019) 364–376.

[4] K. Wang, G.Buschle-Diller, R. D. K. Misra, Chitosan-based injectable hydrogels for biomedical applications, *Mater. Technol.*, 30 (2015) 198-205.

[5] K. Wang, S. Lin, K. C. Nune, R. D. K. Misra, Chitosan-gelatin-based microgel for sustained drug delivery, Mater. Technol., 27 (2016) 441-453.

[6] S. S. Patil, R. D. K. Misra, The significance of macromolecular architecture in governing structure-property relationship for biomaterial applications : an overview, *Mater. Technol.*, 33 (2018) 364-386.

[7] M. A. Abureesh, A. A. Oladipo, M. Gazi, Facile synthesis of glucose-sensitive

chitosan – poly (vinyl alcohol) hydrogel : Drug release optimization and swelling properties, *Int. J. Biol. Macromol.,* 90 (2016) 75-80.

[8] R. Dend, Y. Yue, F. Jin, Y. Chen, H. F. Kung, M. C. M. Lin, C. Wu, Revisit the complexation of PEI and DNA-How to make low cytotoxic and highly efficient PEI gene transfection non-viral vectors with a controllable chain length and structure, *J. Control.* Release, 140 (2009) 40-46.

[10] A. A. Umaredkar, P. V Dangre, D. K. Mahapatra, and M. Dhabarde, Fabrication of chitosan-alginate polyelectrolyte complexed hydrogel for controlled release of cilnidipine : a statistical design approach, *Mater. Technol.,* 35 (2020) 697-707.

[11] A. Thomas, J. Bera, Fabrication and characterization of polymer- infiltrated glass ceramic-titania scaffold for bone substitution, *Mater. Technol.,* 35 (2020) 168-178.

[12] M. Goldshtein, S. Shamir, E. Vinogradov, A. Monsonego, and S. Cohen, Co-assembled Ca^{2+} Alginate-Sulfate Nanoparticles for Intracellular Plasmid DNA Delivery, *Mol. Ther. Nucleic Acid,* 16 (2019) 378-390.

[13] I. Priyan, S. Fernando, W. Lee, E. G. Han, and G. Ahn, Alginate-based nanomaterials : Fabrication techniques , properties , and applications, *Chem. Eng. J.,* 391 (2020) 12-14.

[14] H. M. Kropp, S. L. Durr, C. Peter, K. Diiederichs, A. Marx, Snapshots of a

modified nucleotide moving through the confines of a DNA polymerase, *PNAS. J.*, 115 (2018) 9992-9997.

[15] T. J. Krogh, J. M. Jensen, C. Kaleta, Impact of Chromosomal Architecture on the Function and Evolution of Bacterial Genomes, Frontires in microbiliogy, 9 (2019) 1-15.

[16] P. P. Arayici, T. Acar, and M. Karahan, Transcription and translation of DNA molecule, *OMICS International eBooks*, 15 (2014) 1-27.

[17] A.Psifidi, C.Dovas, G. Bramis, T. Lazou, C. L. Russel, G. Arsenos, G. Banos, Comparison of Eleven Methods for Genomic DNA Extraction Suitable for Large-Scale Whole-Genome Genotyping and Long-Term DNA Banking Using Blood Samples, Plos. J., 10 (2015) 1-18.

[18] J. C. Venter, M. D. Adams, E. W. Myers, P. W. Li, R. J. Mural, G. G. Sutton, The Sequence of the Human Genome, *Science advanced J.*, 291 (2001) 1304-1351.

[19] D. C. Cortes, L. Griffiths, Methods for extracting genomic DNA from whole blood samples : current perspectives, *Journal of Biorepository Science for applied medicine,* 2 (2014) 1–9.

[20] G. Solanki, Polymerase chain reaction procedure, *International Journal of Pharmacological Research*, 2 (2012) 98-102.

[21] K. Verma, J. Dalal, and S. Sharma, Scientific Concepts of Polymerase Chain

Reaction (PCR), *International Journal of Pharmaceutical sciences and researches,* 5 (2014) 3086-3095.

[22] P. Y. Lee, J. Costumbrado, C. Hsu, and Y. H. Kim, Agarose Gel Electrophoresis for the Separation of DNA Fragments, J. Visualized Experiments, 62 (2012) 1-5.

[23] M. M. Muharram, M. S. Abdelkader, Utilization of gel electrophoreses for the quantitative estimation of digestive enzyme papain, *Saudi. Pharm. J.*, 25 (2017) 359-364.

[24] Q. Chai, Y. Jiao, and X. Yu, Hydrogels for Biomedical Applications: Their Characteristics and the Mechanisms behind Them, *J,. Gels,* 3 (2017) 1-15.

[25] E. M. Ahmed, Hydrogel: Preparation, characterization, and applications: A review, *J. Adv. Res.*, 6 (2015) 105–121.

[26] S. Garg, A. Garg, Hydrogel : Classification , Properties , Preparation and Technical Features, *Asian J. of Bio. Res.*, 6 (2016) 163-170.

[27] W. Laftah, S. Hashim, N. I. Akos, Polymer Hydrogels : A Review Polymer Hydrogels : A Review, *Mater. Technol.,* 50 (2014) 1475-1486.

[28] S. Garg, A. Garg, Hydrogel : Classification , Properties , Preparation and Technical Features, *J. Biomaterial Research,* 2 (2016) 163-170.

[29] L. Griffiths and D. C. Cortes, Methods for extracting genomic DNA from whole blood samples: current perspectives, *J. Biorepository Sci.* 2 (2014) 1-9.

[30] F. M. Carpi, F. Di Pietro, S. Vincenzetti, and F. Mignini, V. Napolioni, Human DNA extraction methods : patents and applications Human DNA Extraction Methods : Patents and Applications, *Pubmed J.*, 5 (2011) 1-7.

[31] T. Sakurai, K. Uchida, N. Kuno, Y. Nagoaka, Development of Nucleic Acid Extraction Technology and Its Product Strategy, *Hitachi Review*, 103 (2005) 70-73.

[32] M. T. Rahman, M. S. Uddin, R. Sultana, A. Moue, and M. Setu, Polymerase Chain Reaction (PCR): A Short Review, *Anwer Khan Modern Medical College Journal* 4 (2013) 30-36.

[33] J. S. Blum, W. M. Saltzman, High Loading Efficiency and Tunable Release of Plasmid DNA Encapsulated in Submicron Particles Fabricated from PLGA Conjugated with Poly-L-lysine, *Journal of Controlled Release*, 129 (2008) 66-72.

[34] A. H. E. Machado, D. Lundberg, A. J. Ribeiro, F. J. Francisco, J. Veiga, M. G. Miguel, B. Lindman, Encapsulation of DNA in Macroscopic and Nanosized Calcium Alginate Gel Particles, *Int. J. Biol. Macromol.*, 29 (2013) 15926-15935.

[35] X. Wen, T. Wang, Z. Wang, L. Li, C. Zhao, Preparation of konjac glucomannan hydrogels as DNA-controlled release matrix, *Int. J. Biol. Macromol.*, 42 (2008)

256-263.

[36] A. A. Oladipo, M. Gazi, and E. Yilmaz, Chemical Engineering Research andDesign Single and binary adsorption of azo and anthraquinone dyes by chitosan-based hydrogel : Selectivity factor and Box-Behnken process design, *Chem. Eng. Res. Des.*, 104 (2015) 264–279.